small t in Figure 2, a calculated value for t_s can be obtained. For nylon 6, t_s is 3.03 mils and for nylon 6-6, t_s is 2.27 mils. This again is in good agreement with the values taken from Figure 2 and that estimated from the photomicrograph in Figure 1.

Conclusion

The dynamic Young's moduli of molded films of two polyamides, nylon 6 and nylon 6-6, decrease with increasing thickness. The modulus of the transcrystalline region in each polymer is higher than that of the bulk phase. Both polyamides appear to reach an asymptotic lower limiting value of E in films 23 mils or thicker. An upper limiting value of E is reached at 2.60×10^{10} dyn/cm^2 for 3-mil thick nylon 6 films and 2.92×10^{10} dyn/cm^2 for 2.5-mil thick nylon 6-6 films. The mechanical response of a combination of the surface and bulk regions can be described quantitatively by a "parallel" model.

Rheological Properties of Anionic Polystyrenes. III. Characterization and Rheological Properties of Four-Branch Polystyrenes

Toshiro Masuda,* Yasuhiko Ohta, and Shigeharu Onogi

Department of Polymer Chemistry, Kyoto University, Kyoto, Japan.
Received August 3, 1971

ABSTRACT: The viscoelastic properties of four-branch polystyrene were measured in the molten state by means of a concentric cylinder-type rheometer over wide ranges of frequency and temperature. The star polymer samples were prepared by coupling narrow-distribution polystyryl anion with $SiCl_4$ and were characterized in terms of molecular weight, molecular weight distribution, and coupling ratio. From the frequency dependence of the storage shear modulus G' and the loss modulus G'', the characteristic parameters in the terminal and rubbery zones were evaluated, and their dependences on molecular weight were compared with those for narrow-distribution linear polystyrene. The zero-shear viscosity η_0 and the elasticity coefficient A_G for the star polymer are generally lower than those for the linear polymer having the same molecular weight. The steady-state compliance J_e^0, on the other hand, is about one decade higher. The entanglement compliance J_{eN}^0 of the star polymer is somewhat higher than that of the linear polymer at lower molecular weights, but approaches the latter at higher molecular weights. The average molecular weight between entanglement loci M_e varies similarly with molecular weight. The effects of molecular weight distribution and branching on the G' *vs.* frequency curve and relaxation spectrum are compared for three typical samples having almost the same molecular weights.

In our previous papers, the viscoelastic properties in the rubbery and flow or terminal zones of anionic polystyrene[1,2] and poly(methyl methacrylate)[3–5] were measured over wide ranges of frequency and temperature, and the results were compared with the predictions of the current molecular theories for viscoelasticity. These studies provided much new information on the effects of molecular weight and its distribution on the rheological properties of amorphous polymers.

The effect of branching on the viscoelastic properties is another important but unsolved problem in polymer science, and is difficult to separate from that of molecular weight distribution. Although many papers on the effect of branching have hitherto been published, in most of these papers either the type, number, or length of the branches has not been well characterized,[6–10] or only viscous properties have been measured for well-characterized samples.[11,12] In order to clarify the effect of branching, branched polymers that are well characterized with respect to type, number, and length of branches as well as molecular weight distribution should be employed as samples. Furthermore, it is highly important to measure not only the viscous but also the elastic properties of these samples over wide ranges of time scale and temperature, because such materials are typical viscoelastic materials and their behavior thus depends strongly upon time scale and temperature. The only study which satisfies such conditions is that by Fujimoto, *et al.*[13] These investigators employed comb-shaped polystyrenes having very narrow distributions of molecular weight, which showed viscoelastic properties quite different from those of the corresponding linear polymers. As is well known, however, there are other types of branched polymers than the comb shaped, such as star shaped and randomly branched polymers.

The present paper deals with the viscoelastic properties of four-branch star polystyrenes of differing molecular weights, comparing the results with those for the corresponding linear polystyrenes of narrow distribution, as reported in the previous papers.[1,2]

(1) S. Onogi, T. Masuda, and K. Kitagawa, *Macromolecules*, **3**, 109 (1970).
(2) T. Masuda, K. Kitagawa, T. Inoue, and S. Onogi, *ibid.*, **3**, 116 (1970).
(3) S. Onogi, T. Masuda, and T. Ibaragi, *Kolloid-Z. Z. Polym.*, **222**, 110 (1968).
(4) T. Masuda, K. Kitagawa, and S. Onogi, *Polym. J.*, **1**, 418 (1970).
(5) S. Onogi, T. Masuda, N. Toda, and K. Koga, *ibid.*, **1**, 542 (1970).
(6) L. H. Tung, *J. Polym. Sci.*, **46**, 409 (1960).
(7) W. L. Peticolas, *ibid.*, **58**, 1405 (1962).
(8) V. C. Long, G. C. Berry, and L. M. Hobbs, *Polymer*, **5**, 517 (1964).
(9) S. Onogi, S. Kimura, T. Kato, T. Masuda, and N. Miyanaga, *J. Polym. Sci., Part C*, **No. 15**, 381 (1966).
(10) W. W. Graessley and J. S. Prentice, *ibid., Part A-2*, **6**, 1887 (1968).
(11) G. Kraus and J. T. Gruver, *ibid. Part A*, **3**, 105 (1965).
(12) D. P. Wyman, L. Elyash, and W. J. Frazer, *ibid., Part A*, **3**, 681 (1965).
(13) T. Fujimoto, H. Narukawa, and M. Nagasawa, *Macromolecules*, **3**, 57 (1970).

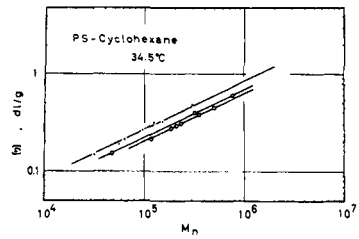

Figure 1. The relation between $[\eta]$ and M_n for the parent (●) and star (○) polystyrenes. The uppermost line corresponds to eq 1.

Experimental Section

Preparation of Star Polystyrene Samples. First, narrow-distribution living polystyrenes were prepared by anionic polymerization at a low temperature near 0° under pressures below 10^{-6} mm, using benzene–tetrahydrofuran (THF) as the solvent and *n*-butyllithium as the initiator. The polymerization procedure was similar to that reported previously.[1] The concentration of the initiator was 0.232 *N* in *n*-hexane.

A part of the polystyryl anion thus prepared was removed and characterized after termination and purification with methanol. This is referred to as the "parent polymer." The remainder was coupled with $SiCl_4$ at room temperature with stirring for about 1 week.[14] After being precipitated and purified with methanol, the polymer was fractionated by precipitation in benzene–methanol systems in order to remove low molecular weight substances. Yields were about 30–60%. The star polymer samples thus prepared were dried in a vacuum oven at 60°.

Determination of Molecular Weights and Intrinsic Viscosity. The number-average molecular weight M_n of the parent and star polymers was determined by the osmotic pressure technique using the high-speed membrane osmometer, Model 502, of Mecrolab Inc. The weight-average molecular weight M_w of two star polymer samples, LB23 and LB11, was determined from light-scattering data. The intrinsic viscosity $[\eta]$ of all samples was measured with dilute solutions in cyclohexane at 34.5° (Θ temperature). In addition, the molecular weight distribution was measured by means of the gel permeation chromatograph (GPC), Model 200, manufactured by Waters Associates Inc. The GPC measurements were carried out at room temperature. By numerical analysis of the GPC charts, the ratio M_w/M_n was evaluated. Since the log $[\eta]$ M *vs.* elution volume curves for the linear and branched polymers are the same straight line,[15] M_w/M_n thus determined appears to be very reliable, as will be further discussed below.

Measurement of Viscoelasticity. The measurements of the viscoelastic properties of the star polymer were carried out with the concentric cylinder type rheometer described in the previous papers.[1-5,16] The frequency of oscillation ranged from 4×10^{-3} to 0.5 Hz. The measuring temperature ranged from 120 to 280°.

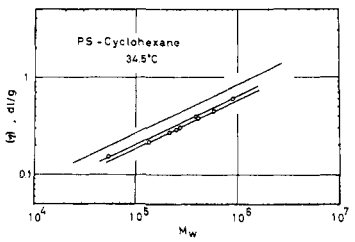

Figure 2. The relation between $[\eta]$ and M_w for the star polystyrenes (○). The uppermost line corresponds to eq 1.

(14) M. Morton, T. E. Helminiak, S. D. Gadkary, and F. Bueche, *J. Polym. Sci.*, **57**, 471 (1962).
(15) Z. Grubisic, P. Rempp, and H. Benoit, *ibid.*, *Part B*, **5**, 753 (1967).
(16) M. Horio, S. Onogi, and S. Ogihara, *J. Jap. Soc. Testing Mater.*, **10**, 350 (1961).

TABLE I
MOLECULAR WEIGHTS AND COUPLING RATIOS OF THE STAR POLYSTYRENE SAMPLES AND THEIR PARENT POLYMERS

Sample	M_n(os)	Parent polymer M_n(os)	Parent polymer $[\eta]_l$[a]	Coupling ratio, P
LB23	772,000	297,000	0.484	2.60
LB18	498,000	147,000	0.321	3.39
LB17	351,000	98,100	0.260	3.58
LB3	320,000	124,000	0.318	2.58
LB16	234,000	64,000	0.209	3.66
LB15	210,000	56,300	0.187	3.74
LB7	187,000			
LB11	119,000	31,900	0.146	3.73
LB8	47,800	15,700		3.04

[a] Subscript l refers to the (linear) parent polymers.

The viscoelastic functions such as the storage shear modulus G' and loss modulus G'' were calculated by use of the general equation given by Markovitz.[17]

Results and Discussion

Characterization of the Star Polystyrenes. In Table I are shown M_n values for the star and parent polystyrenes, the intrinsic viscosities of the parent polymers, and the coupling ratios P (ratio of M_n for the star polymer to that for the corresponding parent polymer). For samples LB23, LB3, and LB8, P is rather low; for the other samples it is higher.

Table II shows the corresponding data for the star polymers. M_n(os) and M_w(ls) in this table are respectively the number- and weight-average molecular weights determined by the osmotic pressure and light-scattering methods. On the other hand, the values of M_w/M_n(GPC) in the fourth column of this table were calculated from the GPC chart. M_w in the fifth column is the product of M_w/M_n(GPC) and M_n(os).

It is evident from Table II that M_w values calculated from M_w/M_n(GPC) agree well with M_w determined by the light-scattering method. This means that although the GPC method gives inaccurate weight-average molecular weights for branched polymers because of the smaller dimensions of the branched polymers in comparison with those of the linear ones, this method nonetheless affords accurate ratios of M_w/M_n.

The intrinsic viscosities $[\eta]_l$ and $[\eta]_b$ are plotted against M_n in Figure 1 and against M_w in Figure 2. The uppermost

TABLE II
MOLECULAR WEIGHTS AND MOLECULAR WEIGHT DISTRIBUTIONS OF THE STAR POLYSTYRENE SAMPLES

Sample	M_n(os)	M_w(ls)	M_w/M_n-(GPC)	M_w	$[\eta]_b$[a]
LB23	772,000	893,000	1.16	893,000	0.611
LB18	498,000		1.16	580,000	0.457
LB17	351,000		1.16	407,000	0.382
LB3	320,000		1.18	378,000	0.394
LB16	234,000		1.17	274,000	0.306
LB15	210,000		1.18	248,000	0.293
LB7	187,000		1.14	213,000	0.273
LB11	119,000	138,000	1.14	135,000	0.216
LB8	47,800		1.12	53,300	0.153

[a] Subscript b refers to the (branched) star polymers.

(17) H. Markovitz, *J. Appl. Phys.*, **23**, 1070 (1952).

straight lines in these figures correspond to the viscosity equation proposed by Altares, *et al.*[18]

$$[\eta]_l = (8.5 \times 10^{-4})M^{0.5} \quad (1)$$

for narrow-distribution polystyrene, and have the slope of 0.5. $[\eta]_l$ for the parent polymer (black circles in Figure 1) is well represented by this equation. However, $[\eta]_b$ for the three branched polymers (LB23, LB3, and LB8) having lower coupling ratios gives the middle straight line of the same slope, and $[\eta]_b$ for the other star polymers of higher coupling ratios gives the bottom line. The intrinsic viscosity for the star polymer, $[\eta]_b$, is thus lower than that for the linear or parent polymer of the same molecular weight, $[\eta]_l$. Moreover, star polymer samples having higher coupling ratios show lower intrinsic viscosities than those having lower coupling ratios.

The straight lines for the star polymers in Figures 1 and 2 can be represented well by the following relations.

$$[\eta]_b = (6.5 \times 10^{-4})M_w^{0.5} \text{ (for LB23, LB3, and LB8)} \quad (2a)$$

$$[\eta]_b = (5.9 \times 10^{-4})M_w^{0.5} \text{ (for the others)} \quad (2b)$$

$$[\eta]_b = (7.0 \times 10^{-4})M_n^{0.5} \text{ (for LB23, LB3, and LB8)} \quad (3a)$$

$$[\eta]_b = (6.4 \times 10^{-4})M_n^{0.5} \text{ (for the others)} \quad (3b)$$

According to Zimm and Stockmayer,[19] the ratio of the mean-square radius of gyration $\langle s^2 \rangle$ for a star-branched polymer having branches of the same length to that for the corresponding linear polymer is given by

$$g_s^2 = \langle s^2 \rangle_b / \langle s^2 \rangle_l = (3P - 2)/P^2 \quad (4)$$

Figure 3 shows the relation between $g_\eta^3 = [\eta]_b/[\eta]_l$ and g_s^2 for the star polymers employed in this study. g_η^3 was evaluated from the molecular weights and $[\eta]_b$ given in Table II using eq 1, and g_s^2 from P in Table I using eq 4. The closed and open circles in this figure represent g_η^3 evaluated from M_n and M_w, respectively. The slopes of the two middle straight lines in this figure are 0.7 and 0.9, giving the relation $g_s = g_\eta^{1.7-2.1}$. This relation differs from that of $g_s = g_\eta^3$, which was presented by earlier authors[20,21] for star-shaped polymers and is referred hereafter to as the Zimm–Kilb (ZK) relation. The straight lines corresponding to this ZK relation and the well-known Fox–Flory (FF) relation, $g_s = g_\eta$, for linear polymers are also drawn in Figure 3. The two points for the samples LB23 and LB3 having P values between 3 and 2 are located near the FF line, since these two samples contained large amounts of linear components.

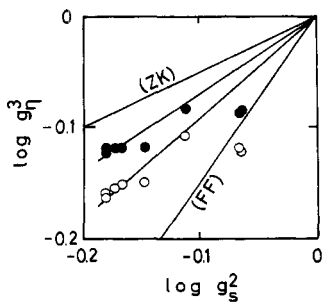

Figure 3. The relation between g_η^3 and g_s^2 for star polystyrenes. g_η^3 was evaluated from eq 1 on the basis of M_n (●) and M_w (○).

(18) T. Altares, Jr., D. P. Wyman, and V. R. Allen, *J. Polym. Sci., Part A*, 2, 4533 (1964).
(19) B. H. Zimm and W. H. Stockmayer, *J. Chem. Phys.*, 17, 1301 (1949).
(20) B. H. Zimm and R. W. Kilb, *J. Polym. Sci.*, 37, 19 (1959).
(21) T. A. Orofino and F. Wenger, *J. Phys. Chem.*, 67, 566 (1963).

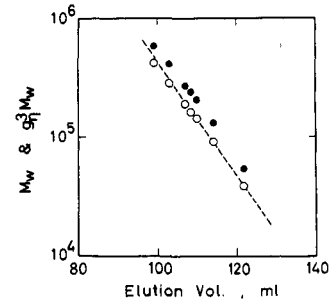

Figure 4. The logarithms of M_w (●) and $g_\eta^3 M_w$ (○) plotted against elution volume for the star polystyrenes. The broken line indicates the relation between M_w and elution volume for the linear polystyrenes.

In Figure 4 are shown the GPC calibrations for star-shaped polystyrenes having coupling ratios higher than 3.0 (closed circles), as well as for narrow-distribution linear polystyrenes (broken line). The open circles in this figure represent $g_\eta^3 M_w$ instead of M_w for the star polystyrenes and fall exactly on the broken line for the linear polystyrenes. Similar results have been reported by previous authors.[15] It follows from these results that our determination of M_w as the product of M_w/M_n(GPC) and M_n(os) is valid.

Temperature and Frequency Dependences of Viscoelastic Functions. As in the case of narrow-distribution linear polystyrene reported in the previous papers,[1,2] log G' *vs.* log ω (angular frequency) curves as well as similar curves for the loss modulus G'' for the star polymers at different temperatures could always be superposed into the respective master curves at 160° by horizontal shifting without correction for absolute temperature T or density ρ. The shift factor a_T for the star polymer is quite the same as that for the linear polymer, provided the molecular weight is higher than the so-called critical molecular weight M_C. This means that the star polymer has the same fractional free volume f and thermal expansion coefficient α_f as the linear polymer, regardless of the difference in the number of chain ends. Such minor differences in the number of chain ends seem not to cause any change in free volume. Similar results were reported by Fujimoto, *et al.*,[13] for comb-shaped polystyrenes, which had more branches or chain ends than the star-shaped polymers employed in this study.

The master curves of log G' *vs.* log ω and log G'' *vs.* log ω for the star polymers are shown in Figures 5 and 6. All the curves cover the flow or terminal, rubbery, and transition

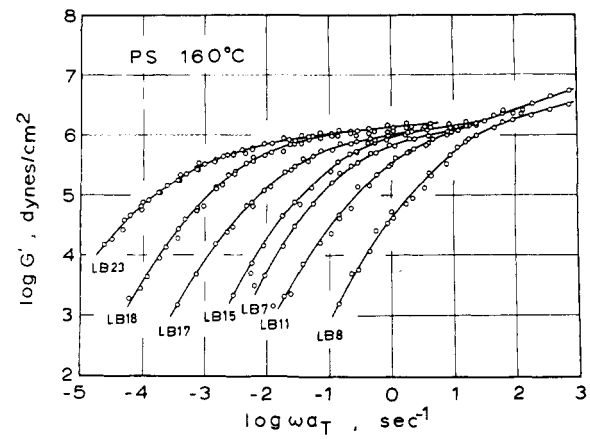

Figure 5. Master curves of G' for star polystyrenes of differing molecular weights. The reference temperature is 160°.

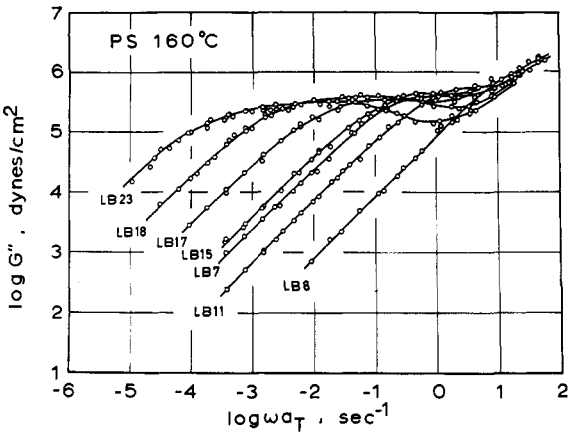

Figure 6. Master curves of G'' for star polystyrenes of differing molecular weights. The reference temperature is 160°.

zones. In the rubbery zone, both G' and G'' are independent of molecular weight and number of branches. The terminal zone shifts progressively to the low-frequency side and the rubbery plateau becomes longer and longer as the molecular weight increases. G' in the termonal zone is proportional to ω^2. The G'' curves for the high molecular weight samples show clear peaks in the rubbery zone, but the peaks become broader and eventually disappear as the molecular weight decreases. G'' in the terminal zone is proportional to ω.

Viscoelastic Parameters in the Terminal Zone. In Figure 7 the molecular weight (M_w) dependence of the zero-shear viscosity η_0 for the star polymer is compared with that for the linear polymer (broken line), where η_0 is defined as follows

$$\eta_0 = \lim_{\omega \to 0} [G''(\omega)/\omega] \tag{5}$$

In this figure, the open and closed circles are for star-shaped samples having coupling ratio P above and below 3.0, respectively. The star polymer shows lower η_0 over the entire range of molecular weight covered by this study. η_0 for samples of higher molecular weights and coupling ratios, however, can be represented by a straight line having a slope of 4.5, and possibly exceeds η_0 for the linear polymers at molecular weights higher than 1×10^6.[11] Figure 8 shows the molecular weight dependence of the elasticity coefficient A_G defined by the following equation[22]

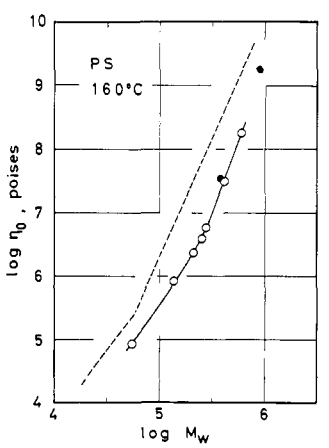

Figure 7. Molecular weight dependence of zero-shear viscosity η_0 for the star polystyrenes at 160°.

(22) J. D. Ferry, "Viscoelastic Properties of Polymers," 2nd ed, Wiley, New York, N. Y., 1970.

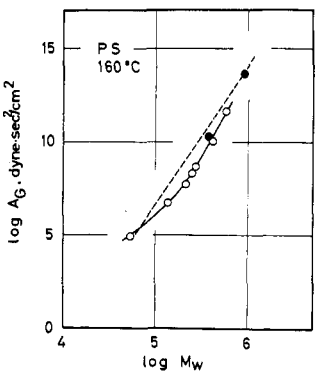

Figure 8. Molecular weight dependence of elasticity coefficient A_G for the star polystyrenes at 160°.

$$A_G = \lim_{\omega \to 0} [G'(\omega)/\omega^2] \tag{6}$$

In this figure, the solid line again represents the results for the star polymer, while the broken line shows those for the linear polymer. The latter has a slope of 7.5 and joins with the former at the highest and lowest molecular weights. The open and closed circles indicate respectively the values for star polymers having P above and below 3.0, as in Figure 7, and the slope of the straight line at higher molecular weights is 9.0.

As seen from these figures, the molecular weight dependence curves of η_0 and A_G for the star polystyrenes increase their slopes rather rapidly at around $M_w = 1.5 \times 10^5$. However, it is difficult to conclude that this molecular weight value is the critical molecular weight for entanglement couplings, because sample LB11, having a lower M_w of 119,000, still shows the rubbery plateau as seen from the G' curve in Figure 5. This behavior is not clear at present, but it may be attributable to the fact that the entanglement spacing expands with decreasing molecular weight, as will be discussed below.

Figure 9 shows the ratio of the zero-shear viscosity for narrow-distribution linear polystyrenes, η_l, to that for the star polystyrenes, η_b, logarithmically plotted against the logarithm of (M_s/M_e), where M_s and M_e are the molecular weight of a branch (M_n of the parent polymer) and the average molecular weight between entanglement loci for the linear polystyrene (18,000, as reported in our previous paper[1]), respectively. The broken line in this figure has the slope of -0.8 and was drawn to be consistent with the two straight lines for the linear and star polymers in Figure 7. The curve indicated by the solid line appears to fit the experimental points rather well. The extrapolated values of (M_s/M_e) at $\log(\eta_l/\eta_b) = 0$ are roughly estimated to be 60 and 20 from the broken and solid lines, respectively. From these values, the

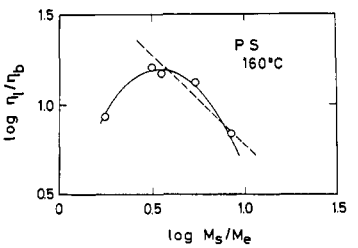

Figure 9. The ratio of the zero-shear viscosities for the linear and star polystyrenes, logarithmically plotted against the logarithm of the ratio of the molecular weight of a branch to the entanglement spacing of linear polystyrenes.

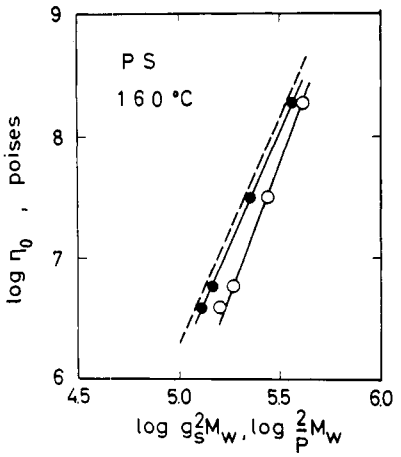

Figure 10. The zero-shear viscosity η_0 logarithmically plotted against the corrected molecular weights $g_s^2M_w$ (○) and $2M_w/P$ (●). The broken line represents the data for narrow-distribution linear polystyrenes.

molecular weight where η_b exceeds η_l can be estimated to be 1.2×10^6 and 4×10^6.

The zero-shear viscosity η_0 is logarithmically plotted against the corrected molecular weight, $g_s^2M_w$, instead of M_w, in Figure 10. Such a plot is based on the theoretical consideration of Bueche that the ratio of the viscosity of branched polymers to linear ones depends only on the radius of gyration.[23] As is evident from this figure, the plot of log η_0 *vs.* log $g_s^2M_w$ for star polystyrenes (open circles) can be represented by a straight line having a slope of 4.5, which does not coincide with that for linear polymers. It is noteworthy that the slopes of the log η_0 *vs.* log M_w and log $g_s^2M_w$ curves are both 4.5, very near 4.3, which is the slope of the log η_0 *vs.* log M_w curves for comb-shaped polystyrene having a constant number of branches.[13]

The relation between log η_0 and log $(2M_w/P)$ is also shown in Figure 10, by closed circles. $2M_w/P$ corresponds to an end-to-end contour length of the star-shaped polymer chains. The slope of the straight line in this figure is 3.7. This slope is the same as that of the corresponding curve for linear polystyrenes (broken line),[1] but the values themselves are slightly lower than in the latter case.

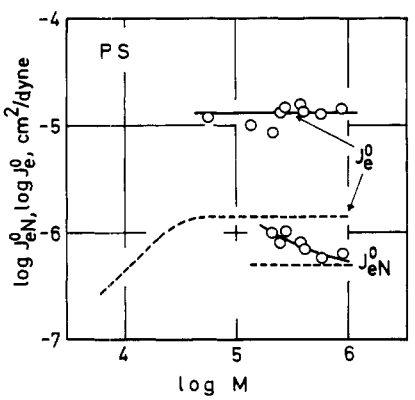

Figure 11. A comparison of the molecular weight dependences of J_e^0 and J_{eN}^0 for the star and linear polystyrenes.

(23) F. Bueche, *J. Chem. Phys.*, **40**, 484 (1964).

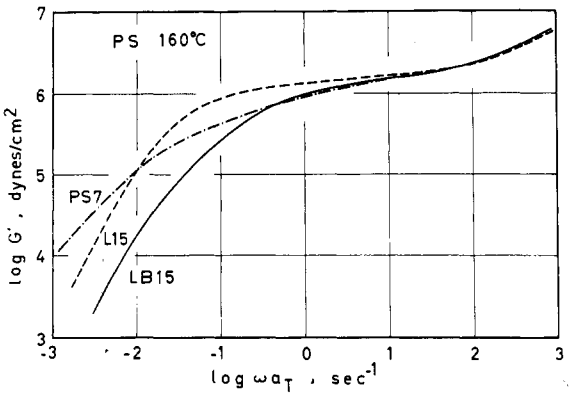

Figure 12. A comparison of G' curves for the narrow-distribution, broad-distribution, and four-branch star polystyrenes.

Another parameter which determines the terminal zone is the steady-state compliance J_e^0 defined by the following

$$J_e^0 = \lim_{\omega \to 0} [G'(\omega)/G''^2(\omega)] = A_G/\eta_0^2 \qquad (7)$$

In Figure 11, J_e^0 for the star polymer (open circles) is compared with that for the linear polymer (broken line). It is surprising to note that the value for the star polymer is about one decade higher than that for the linear polymer. This is the most outstanding difference between the star polymer and the linear one. Quite a similar result was reported by Fujimoto, *et al.*,[13] for comb-shaped polystyrene. Accordingly, it can be concluded that branched polymers, or at least comb- and star-shaped ones, show much higher J_e^0 values than their linear counterparts.

Viscoelastic Parameters in the Rubbery Zone. The most important parameters to determine the rubbery zone are the quasiequilibrium or entanglement modulus G_{eN}^0, the entanglement compliance J_{eN}^0, and the average molecular weight between entanglement loci, M_e

$$G_{eN}^0 = \frac{2}{\pi}\int_{-\infty}^{a} G''(\omega)\mathrm{d}\ln\omega = 1/J_{eN}^0 \qquad (8)$$

$$M_e = g_N\rho RT/G_{eN}^0 = g_N\rho RTJ_{eN}^0 \qquad (9)$$

where g_N is a front factor near unity and ρ is the density of the polymer. These parameters for the narrow-distribution linear polystyrene were discussed in detail in the previous papers.[1,2]

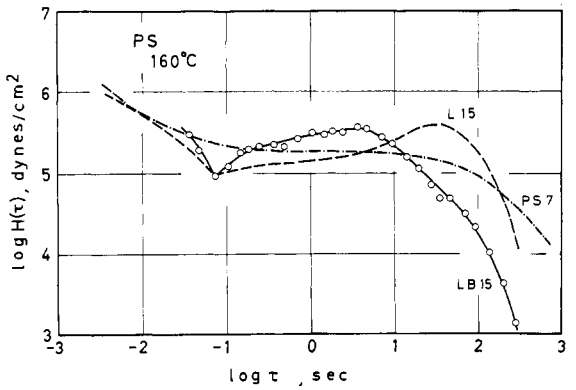

Figure 13. A comparison of relaxation spectra for the narrow-distribution, broad-distribution, and four-branch star polystyrenes.

In Figure 11, the molecular weight dependence of J_{eN}^0 for the star polymer (open circles) is compared with that for the linear polymer (broken line). As is evident from this figure, J_{eN}^0 for the star polymer does not differ greatly from that of the linear polymer, in marked contrast to the case of J_e^0. The value of J_{eN}^0 for the star polymer is somewhat higher than that for the linear one at lower molecular weights, but approaches the latter as molecular weight increases. Correspondingly, M_e for the star polymer is somewhat higher than the average value of 18,000 for the linear polymer,[1] but decreases with increasing molecular weight. These results imply that the center of a star-shaped chain affects entanglements near this point, but that the effect fades as the molecular weight or length of the branches increases. For example, M_e for LB7 (M_w = 213,000) and LB18 (M_w = 580,000) are respectively 35,500 and 19,300.

A Comparison of the Effects of Molecular Weight Distribution and Branching. As was emphasized in the previous papers,[1,2] viscoelastic properties in the rubbery and flow or terminal zones are strongly affected by the molecular weight distribution and blending. On the other hand, they are also affected by branching, as has been described above. It is, therefore, very interesting to compare the effects of molecular weight distribution and branching. Such a comparison has been made using the following three samples of roughly equal M_w

Star LB15	$M_w = 2.48 \times 10^5$, $M_w/M_n = 1.18$
Narrow Distribution L15	$M_w = 2.15 \times 10^5$, $M_w/M_n = 1.00$
Broad Distribution PS7	$M_w = 3.03 \times 10^5$, $M_w/M_n = 1.57$

The last of these samples, PS7, was obtained by bulk polymerization.

Figure 12 shows the frequency dependence curves of G' for these samples. The three samples manifest the same G' in the transition zone, but the rubbery plateau of L15 alone is very flat and much longer than that of LB15. The G' curves for LB15 and PS7 are almost identical down to ω = 0.3, and decrease with decreasing frequency in the rubbery zone; but the curve for PS7 decreases more gradually even in the terminal zone. Similar characteristic features of these samples are also clearly seen in their relaxation spectra as determined by Tschoegl's equation[22] (Figure 13). L15 shows a clear peak in the rubbery flow transition region, and LB15 has a broader peak at a shorter relaxation time. PS7 shows no peak.

Notes

On the Conformation of a Segment of Carp Hemoglobin

A. ENGLERT,* J. FURNÉMONT, AND J. LÉONIS

Université Libre de Bruxelles, Chimie Générale I, Brussels, Belgium. *Received May 3, 1971*

Chemical data on the primary structure of proteins being much more abundant than X-ray data, it seems desirable to develop indirect methods of investigation of tertiary structures.

Here we report computer calculations of the conformation of a small segment (residues 118–120, Phe–Pro–Pro) of the α chain of carp hemoglobin (Hb).[1,2]

In homologous proteins of known tertiary structure, horse Hb and whale sperm myoglobin, the corresponding segment is located at the beginning of the H helix[3] with the following sequences of amino acids: Phe–Thr–Pro (residues 117–119) and Phe–Gly–Ala (residues 123–125), respectively. Phenylalanine is the last residue of the nonhelical part GH.

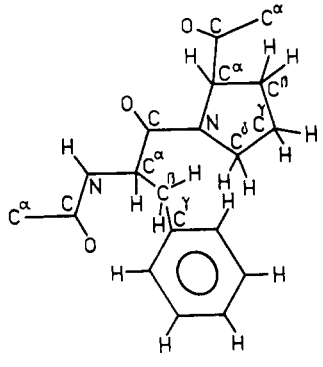

Figure 1. Schematic representation of sequence Phe–Pro.

The presence of the second proline should restrict the number of available conformations for this segment of carp Hb, since it is known that proline modifies the steric maps of the residue preceding it.

Steric maps for a prolyl[4] and an alanyl[5] preceding a prolyl residue in a peptide sequence have been calculated by Schimmel and Flory. New calculations for the alanyl–prolyl sequence were reported during the period of the present investigations by Damiani, De Santis, and Pizzi.[6]

It is to be expected that the steric map of an alanyl residue should be representative of any residue with a β-carbon atom, such as a phenylalanine. We have felt, however, that it was worthwhile to reconsider steric maps for phenylalanyl–prolyl and prolyl–prolyl sequences in order to get a consistent set of results for the potential functions used and also in order to determine the allowed positions of the side chain of phenylalanine.

The theroetical unit Phe–Pro is represented in Figure 1. The geometrical parameters[4,7] and the potential functions are those of Flory,[8] but with hydrogen and carbon treated as individual atoms.

(1) K. Hilse and G. Braunitzer, *Z. Physiol. Chem.*, **349**, 433 (1968).
(2) M. O. Dayhoff, "Atlas on Protein Sequence and Structure," Vol. IV, National Biomedical Research Foundation, Silver Spring, Md., 1969.
(3) M. F. Perutz, *J. Mol. Biol.*, **13**, 646 (1965).
(4) P. R. Schimmel and P. J. Flory, *Proc. Nat. Acad. Sci. U. S.*, **58**, 52 (1965).
(5) P. R. Schimmel and P. J. Flory, *J. Mol. Biol.*, **34**, 105 (1968).
(6) A. Damiani, P. De Santis, and A. Pizzi, *Nature (London)*, **226**, 542 (1970).
(7) P. J. Flory, "Statistical Mechanics of Chain Molecules," Interscience, New York, N. Y., 1969, p 251.
(8) Reference 7, pp 256 and 257.